

6.3 PYROELECTRIC SENSORS

6.3.1 The Pyroelectric Effect

The pyroelectric effect is analogous to the piezoelectric effect, but instead of change in stress displacing electric charge, now it refers to change in temperature causing change in spontaneous polarization and resulting change in electric charge. This effect was named by David Brewster in 1824, but it has been known for more than 2000 years [11].

When the change in temperature ΔT is uniform throughout the material, the pyroelectric effect can be described by means of the *pyroelectric coefficient*, which is a vector p with the equation

$$\Delta P = p\Delta T \quad (6.36)$$

where P is the spontaneous polarization.

This effect is mainly used for thermal radiation detection at ambient temperature (Section 6.3.3). Two metallic electrodes are deposited on faces perpendicular to the direction of the polarization, which yields a capacitor (C_d) acting as thermal sensor. When the detector absorbs radiation, its temperature and hence its polarization changes, thus resulting in a surface charge on the capacitor plates.

If A_d is the area of incident radiation and the detector thickness b is small enough so that the temperature gradient in it is negligible, then the charge induced will be

$$\Delta Q = A_d \Delta P = p A_d \Delta T \quad (6.37)$$

where ΔT is the increment in temperature of the detector. The resulting voltage will be

$$v_o = \frac{pb}{\epsilon} \Delta T \quad (6.38)$$

When the incident radiation is pulsating and has a power P_i , the resulting voltage on the capacitor is

$$v_o = R_v P_i \quad (6.39)$$

where R_v (V/W) is the *responsivity* or voltage sensitivity, given by [11]

$$R_v = \frac{\alpha p}{C_E \epsilon A} \frac{\tau}{\sqrt{1 + (\omega\tau)^2}} \quad (6.40)$$

p = the pyroelectric coefficient for the material

τ = the thermal time constant

C_E = the volumetric specific heat capacity [$\approx Q/(V\Delta T)$] [J/(m³·K)]

ϵ = the dielectric constant

ω = the pulsating frequency for the incident radiation.

The corresponding short-circuit current is

$$i_{sc} = R_i P_i \quad (6.41)$$

where R_i (A/W) is the *current responsivity*, given by

$$R_i = \omega C_d R_v = \frac{\alpha p}{C_E b} \frac{\omega \tau}{\sqrt{1 + (\omega \tau)^2}} \quad (6.42)$$

which is a high-pass response for frequencies above that determined by the thermal constant of the material. R_v has a bandpass response: (6.40) is a low-pass response because of the thermal time constant, but the device responds only to temperature changes and, hence, there is no dc response. The upper corner frequency for commercial sensors is from 0.1 Hz to above 1 Hz (Figure 6.21). The voltage mode usually yields the best signal-to-noise ratio. The current mode yields a larger output signal and has a flatter frequency response.

As for other radiation detectors, pyroelectric sensors are also sensitive to thermal noise. The *noise equivalent power* (NEP) is the equivalent input power yielding an output response that in a given bandwidth equals that of thermal fluctuations in the detector [12]. The detectivity is $D = 1/\text{NEP}$. The NEP depends on wavelength, operating frequency, temperature, and noise bandwidth (usually 1 Hz). For an ideal detector with area A_d cm², at ambient temperature the NEP is about $5.5 \times 10^{-11} \sqrt{A_d}$ (W/√Hz). The D^* (D -star) parameter normalizes the NEP to a given constant area,

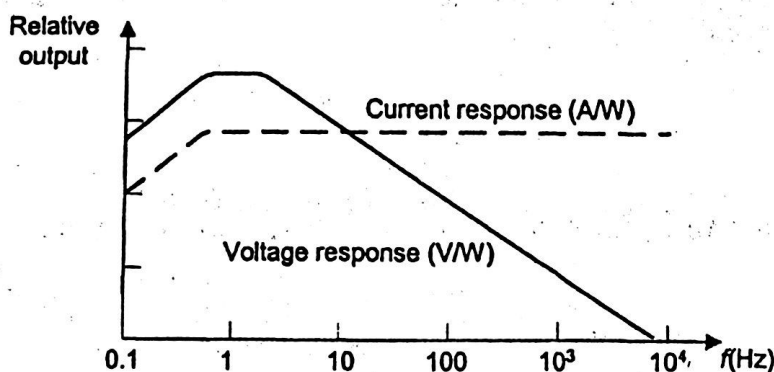


Figure 6.21 Frequency response of pyroelectric sensors in voltage mode (R_v) and current mode (R_i).

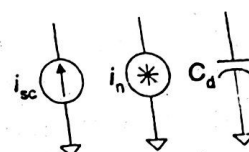


Figure 6.22 Equivalent circuit for a pyroelectric sensor including thermal noise.

$$D^* = \frac{\sqrt{A_d}}{\text{NEP}} \quad (6.43)$$

Figure 6.22 shows the equivalent circuit for a noisy but otherwise ideal pyroelectric sensor. The star symbol for the current generator modeling thermal noise means that it is a random signal (Section 7.4).

6.3.2 Pyroelectric Materials

Given that pyroelectricity, like piezoelectricity, is also based on crystal anisotropy, many of the piezoelectric materials are also pyroelectric. Ten of the 21 noncentrosymmetrical crystallographic classes have a polar axis of symmetry. All of them display pyroelectric properties.

There are two groups of pyroelectric materials: linear and ferroelectric. The polarization of linear materials cannot be changed by inverting the electric field. This group includes materials such as tourmaline, lithium sulfate, and cadmium and selenium sulfides. Some ferroelectric materials with pyroelectric properties are lithium tantalate, strontium and barium niobate, lead zirconate-titanate, and triglycine sulfate (TGS). Some polymeric materials such as polyvinylidene (PVF₂ or PVDF) are also pyroelectric.

Pyroelectric properties disappear at the Curie temperature. For ferroelectric ceramics, the polarization is induced during manufacturing as described in Section 6.2.2.

According to (6.40) the ideal pyroelectric material should simultaneously display a high pyroelectric coefficient, a low volumetric specific heat capacity, and a low permittivity. Table 6.8 lists these parameters for some common pyroelectric materials.

TABLE 6.8 Some Parameters for Common Pyroelectric Materials

Material	Pyroelectric Coefficient (nC/cm ² ·K)	Relative Permittivity	Specific Heat (J/cm ³ ·K)
Triglycine sulfate, TGS	40	35	2.5
Lithium tantalate, TaO ₃ Li	19	46	3.19
Strontium and barium niobate, SBN	60	400	2.34
PVDF	3	12	2.4

6.3.3 Radiation Laws: Planck, Wien, and Stefan–Boltzmann

We can measure the surface temperature of a heated target by allowing its emitted radiation to be absorbed by a pyroelectric detector, which increases its temperature. Thermocouples (thermopiles), thermistors, RTDs, and photoconductors also suit noncontact temperature measurement.

Any body at a temperature greater than 0 K radiates an amount of electromagnetic energy that depends on its temperature and physical properties. At temperatures above 500°C, the emitted radiation is visible. Below 500°C, including ambient temperatures, infrared radiation predominates so that only heat energy is perceived.

In order to study the emission of energy radiating from a body, we consider first its absorption. Of the overall energy received by a body, part is reflected, part is diffused in all directions, part is absorbed, and part is transmitted (i.e., goes through the body). We give the name “blackbody” to a theoretical body that absorbs all the energy incident on it (thereby increasing its temperature). A closed cavity with black walls and controlled temperature, and where only a small aperture is provided, behaves approximately as a blackbody.

At any temperature all bodies emit radiation and absorb that coming from other bodies in their environment. If all bodies are not at the same temperature, the hotter ones will cool and the colder ones will heat, so radiation is enough to reach thermal equilibrium (heat conduction and convection are not required). When equilibrium is reached, all bodies emit as much radiation as they receive. Therefore the bodies emitting more radiation are those that also absorb more, and hence a blackbody is also the best radiation emitter (heat sinks are black). Greenhouses rely on materials that are transparent to visible light but opaque to infrared radiation emitted by bodies heated by that incident light.

The ratio between the energy emitted by a given body per unit area per unit time and that emitted by a blackbody under the same conditions is the *emissivity* of that body ε . For a blackbody, $\varepsilon = 1$. The emissivity depends on the wavelength, the temperature, the physical state, and the chemical characteristics of the surface. For example, unoxidized aluminum has $\varepsilon = 0.02$ at 25°C and $\varepsilon = 0.06$ at 500°C; oxidized aluminum has $\varepsilon = 0.11$ at 200°C and $\varepsilon = 0.19$ at 600°C.

The energy W_λ emitted by the blackbody per unit time, per unit area, at a given wavelength λ and temperature T , is given by Planck's law,

$$W_\lambda = \frac{c_1}{\lambda^5 [\exp(c_2/\lambda T) - 1]} \text{ W cm}^2/\mu\text{m} \quad (6.44)$$

where

$$c_1 = 2\pi c^2 h = 3.74 \times 10^4 \text{ W}\cdot\mu\text{m}^4/\text{cm}^2$$

$$c_2 = hc/k = 1.44 \text{ cm}\cdot\text{K}$$

$h = 0.655 \times 10^{-33} \text{ W}\cdot\text{s}^2$ is Planck's constant

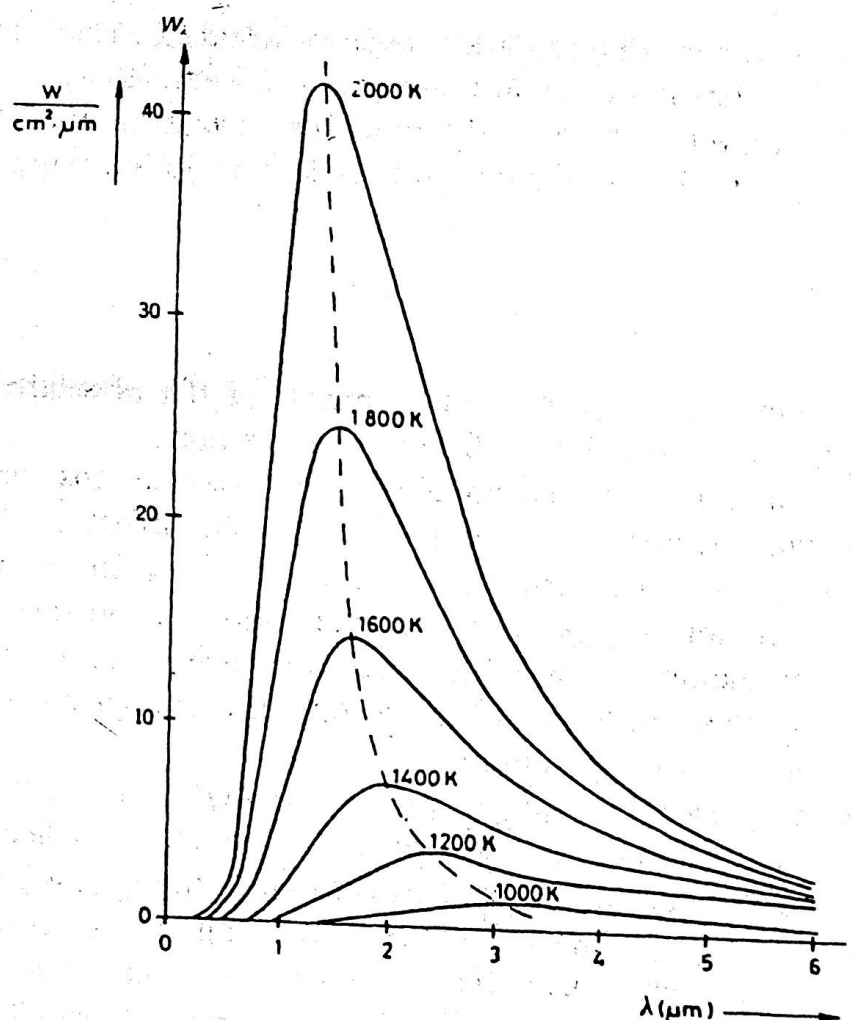


Figure 6.23 Power flux per unit area emitted by the blackbody at different temperatures and at different wavelengths (Planck's law). The dashed line passes through the maximums (Wien's law).

$$k = 1.372 \times 10^{-22} \text{ W}\cdot\text{s/K}$$

is Boltzmann's constant
 $c \approx 300 \text{ Mm/s}$ is the velocity of light.

Figure 6.23 shows the shape of (6.44) for different values of T (in kelvins). The emissivity of real bodies depends on the wavelength, and we have

$$W_{\lambda r} = \epsilon_{\lambda, T} W_{\lambda} \quad \text{and} \quad (6.45)$$

The maximal emitted power for a blackbody is at a wavelength

$$\lambda_{\max} = \frac{2896 \text{ K}\cdot\mu\text{m}}{T} \quad (6.46)$$

which is the equation for Wien's displacement law (to honor the man who discovered it before Planck's law was discovered). It indicates that the maximum is obtained at a wavelength that decreases for increasing temperatures. For example, the human body, with an assumed surface temperature of 300 K, has its

perature is 6000 K, has its maximal emission at 483 nm (blue).

The total flux power emitted by the blackbody per unit area is obtained by integrating (6.44) for all wavelengths. In a half-plane (solid angle 2π), the total emitted flux is

$$W = \sigma T^4 \quad (6.47)$$

which shows a dependence on the fourth power of the absolute temperature. $\sigma = 5.67 \text{ pW/cm}^2 \cdot \text{K}^4$ is the Stefan–Boltzmann constant.

When this radiation arrives at an object, part of it is absorbed. When the absorption is high, the increase in temperature of the object can be significant. This is the principle of operation for thermal detectors: thermopiles and bolometers (RTD, thermistors, pyroelectric detectors). In contrast, quantum detectors (photoconductors, photovoltaic detectors) are based on the generation of electrons by incident photons, which results in a change in resistance or in the contact voltage of a *p*–*n* junction.

In practice, the presence of water vapor, CO₂ and ozone in the air, the dispersion due to dust particles, smoke, and so on, results in a decrease between the radiation emitted and that detected. In addition, the emissivity of the target may be unknown or may change because of varying surface conditions. Two-color or ratio pyrometers solve these problems by measuring two different wavelengths emitted by the target. If those wavelengths are close enough to undergo the same (undesired) variations, the ratio between the signal outputs changes only when the temperature changes at the target. The two signals needed can be obtained by a beam-splitting mirror and matched detectors or by a filter wheel and a single detector. The detailed design of radiometric systems can be found in reference 13.

6.3.4 Applications

The most common application for the pyroelectric effect is the detection of thermal radiation at ambient temperature. It has been applied to pyrometers (noncontact temperature meters in furnaces, melted glass or metal, films, and heat loss assessment in buildings) and radiometers (measurement of power generated by a radiation source). Other applications are IR analyzers (based on the strong absorption of IR by CO₂ and other gases), intruder and position detection, automatic faucet control, fire detection, high-power laser pulse detection, and high-resolution thermometry (6 μK) [14]. Medical thermometers that measure ear temperature detect infrared radiation from the eardrum and surrounding tissue.

Undesirable parasitic charges may neutralize the surface charge induced in the electrodes by desired temperature changes in the detector due to incident radiation. Thus the incident radiation must be modulated, usually by a low-frequency optical chopper that alternatively faces the detector to radiation from

Characteristic	Unit	P3782 ^a	406 ^b
Window material	mm	2	2
Sensing area diameter	μm	2–20	2–15
Optical bandwidth	V/W	1500 ^c	275 ^d
Voltage responsivity	$\text{pW}/\sqrt{\text{Hz}}$	850 ^c	500 ^d
NEP	$\text{cm}^2\sqrt{\text{Hz}}/\text{W}$	$2.2 \times 10^{-8}\text{c}$	$1.7 \times 10^{-8}\text{d}$
D^*	$^\circ\text{C}$	–20 to 60	–55 to 125
Operating temperature range	ms	100	0.2
Rise time (0–63 %)	$^\circ\text{C}/^\circ\text{C}$	0.2	0.2
Temperature coefficient of sensitivity, max.			

^aHamamatsu.

^bEltec.

^cAt 1 Hz.

^dAt 10 Hz.

the target and from an object at ambient temperature. A coherent detector synchronous with the chopper eliminates ambient noise. An alternative technique to reduce bulk or common mode effects uses dual-element, series-opposed detectors.

Pyroelectric sensors are faster than other thermal detectors (thermocouples, thermistors) because they are thin, have high sensitivity, and do not need to reach thermal equilibrium with the radiation source because they detect temperature gradients. This makes them appropriate for imaging by scanning the surface to be detected, as used in infrared thermography (thermal imaging—first demonstrated by J. Herschel in 1840) and applied in nondestructive testing, hot spot monitoring, printed circuit testing, and night vision. Placing the sensor at the focus of a parabolic mirror or a Fresnel lens increases its range to tens of meters. Linear arrays can discriminate targets according to the sequence of elements that are activated.

The detector can be suspended, supported by Mylar®, or mounted in a substrate that can be either thermally conductive or insulating. Because all pyroelectric materials are piezoelectric, these detectors have hermetically sealed packages (sometimes even with an internal vacuum), thus reducing the effects of air movements. Table 6.9 lists some parameters for two pyroelectric detectors suitable for the detection of a human body.

6.4 PHOTOVOLTAIC SENSORS

6.4.1 The Photovoltaic Effect

When the internal photoelectric effect discussed for photoconductors (Section 2.6) occurs in a *p*–*n* junction, it is possible to obtain a voltage that is a function

of the incoming radiation intensity. The photovoltaic effect is the generation of an electric potential when the radiation ionizes a region where there is a potential barrier. It was discovered by E. Becquerel in 1839. D. M. Chapin, C. S. Fuller, and G. L. Pearson invented silicon photovoltaic cells in 1954.

When a *p*-doped semiconductor (doped with acceptors) contacts an *n*-doped semiconductor (doped with donors), because of the thermal agitation there are electrons that go into the *p* region and "holes" that move into the *n*-region. There they recombine with charge carriers of opposite sign. As a result, at both sides of the contact surface there are very few free charge carriers. Also the positive ions in the *n* region and the negative ions in the *p* region, fixed in their positions in the crystal structure, produce an intense electric field that opposes the diffusion of additional charge carriers through this potential barrier. This way an equilibrium is attained between the diffusion current and the current induced by this electric field. By placing an external ohmic connection on each semiconductor, no voltage difference is detected because the internal difference in potential at the junction is exactly compensated by contact potentials in the external connections to the semiconductor.

Figure 6.24 shows that radiation whose energy is larger than the semicon-

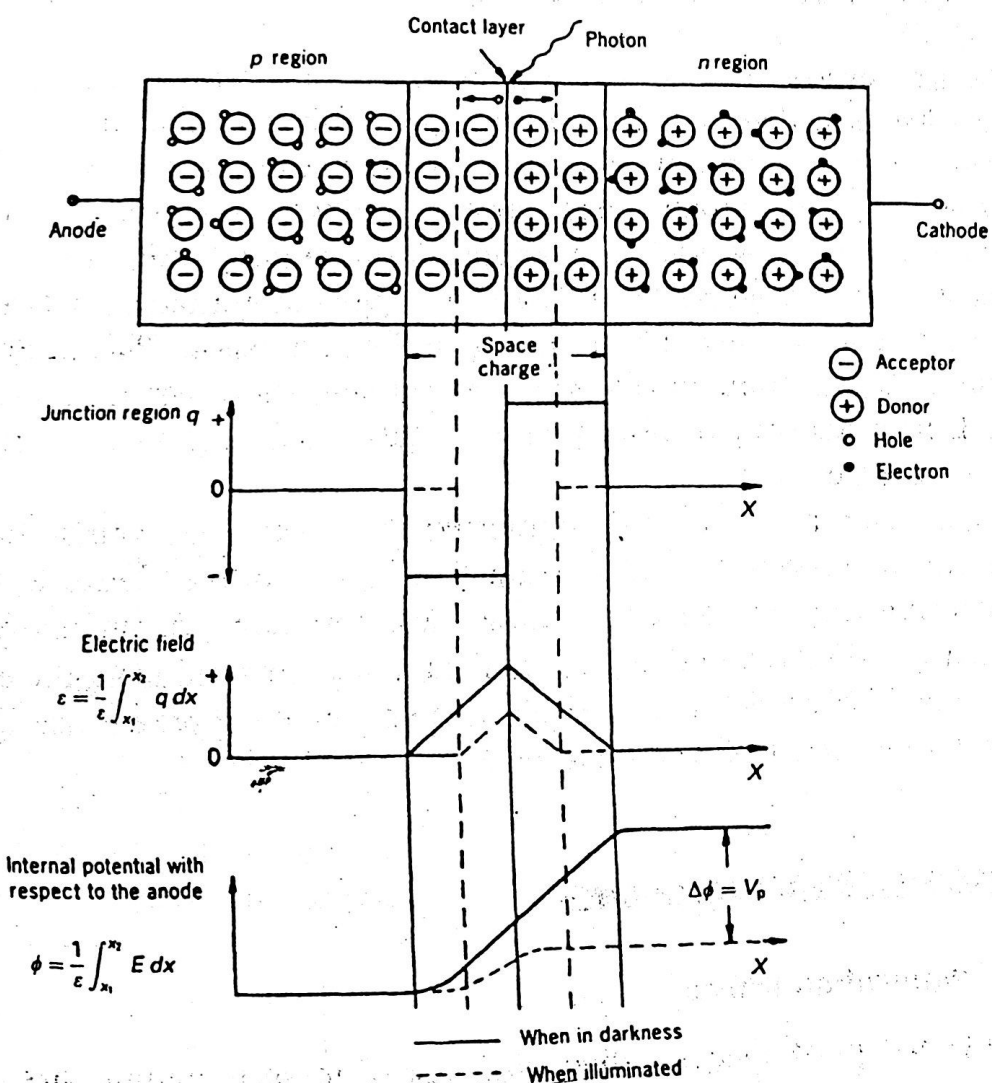


Figure 6.24 Photoelectric effect in a *p*-*n* junction.

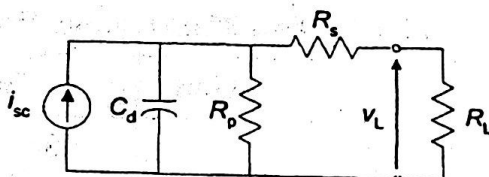


Figure 6.25 Equivalent simplified circuit for a photovoltaic detector. i_{sc} is the short-circuit current, R_p is the parallel resistance, R_s is the output series resistance, and C_d is the junction capacitance. R_L is the load resistance.

ductor band gap generates additional electron–hole pairs that are driven by the electric field in the open circuit p – n junction. The accumulation of electrons in the n region and of holes in the p region results in a change in contact potential V_P that can be measured by means of external connections to a load resistance. This open-circuit voltage increases with the intensity of the incident radiation, until a saturation point is reached (the limit is the band-gap energy). If the contacts are short-circuited, the current is proportional to the irradiation for a broad range of values. Figure 6.25 shows the simplified equivalent circuit.

6.4.2 Materials and Applications

In addition to p – n junctions, there are other methods that produce a potential barrier, but p – n junctions are by far the most common one. If the p – n junction is between semiconductors of the same composition, then it is called a *homojunction*. Otherwise it is called a *heterojunction*.

We select materials for the particular wavelength to be detected, as discussed in Section 2.6 for LDRs. In the visible and near-infrared regions, silicon and selenium are used. Silicon is in the form of homojunctions. Selenium in the form of a selenium layer (p) covering cadmium oxide (n). For silicon sometimes an intrinsic (nondoped) silicon region is added between the p and n regions (p – i – n detectors). This results in a wider depletion region, which yields a better efficiency at large wavelengths, faster speed, and lower noise and dark current. At other wavelengths, germanium, indium antimonide (SbIn), and indium arsenide (AsIn), among others, are used.

Photovoltaic detectors offer better linearity, are faster, and have lower noise than photoconductors, but they require amplification. For large-load resistors, the linearity decreases and the time of response increases. Table 6.10 gives some characteristics for two general purpose photovoltaic cells.

Photovoltaic detectors are used either in applications where light intensity is measured or in applications where light is used to sense a different quantity. They are used, for example, in analytical instruments such as flame photometers and colorimeters, in infrared pyrometers, in pulse laser monitors, in smoke detectors, in exposure meters in photography, and in card readers. Commercial models are available consisting of a matched emitter-detector

TABLE 6.10 Some Characteristics for Two Photovoltaic Detectors

Characteristic	Unit	S639 ^a	J12-18C-R01M ^b
Detector material		Si	AsIn
Sensing area diameter	mm	20	1
Wavelength with maximal sensitivity	μm	0.85	3.6
Responsivity	A/W	0.45	0.7
NEP	pW/√Hz	1	70
D*	cm√Hz/W	2×10^{12}	—
Shunt resistance ^c	Ω	10^4	20
Junction capacitance	nF	100	0.4
Response time (10–90 %)	μs	200	—
Operating temperature range	°C	–10 to 60	22
Short-circuit current for 100 lx	μA	180	—
Open circuit voltage for 100 lx	V	0.3	—

^aHamamatsu.^bEG&G Optoelectronics.^cReverse voltage 10 mV.

6.5 ELECTROCHEMICAL SENSORS

Potentiometric electrochemical sensors yield an electric potential in response to a concentration change in a chemical sample. Amperometric sensors use an applied voltage to yield an electric current in response to a concentration change in a chemical sample. They are not self-generating sensors and are described elsewhere [15, 16].

Ion-selective electrodes (ISEs) are potentiometric sensors based on the voltage generated in the interface between phases having different concentrations. This is the same principle for voltaic cells. Assume that there is only one ion species whose concentration changes from one phase to another, or that there are more ions but a selective membrane allows only one specific ion to go through it. Then the tendency for that ion to diffuse from the high-concentration region to the low-concentration region is opposed by an electric potential difference due to the ion electric charge. When we have equilibrium between both forces (diffusion and electric potential), the difference in potential is given by the Nernst equation (first reported in 1899),

$$E = \frac{RT}{zF} \ln \frac{a_{i,1}}{a_{i,2}} \quad (6.48)$$

where $R = 8.31 \text{ J/(mol}\cdot\text{K)}$ is the gas constant, T is the temperature in kelvins, z is the valence for the ion, $F = 96,500 \text{ C}$ is Faraday's constant, and a_i is the ion activity. For a liquid solution, activity is defined as

$$a_i = C_i f_i \quad (6.49)$$

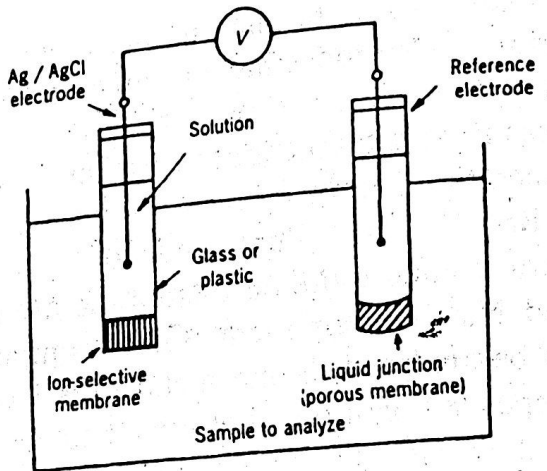


Figure 6.26 Measurement arrangement using an ion-selective electrode (ISE).

where C_i is the concentration for species i , and f_i is the activity coefficient, which describes the extent to which the behavior of species i diverges from the ideal, which assumes that each ion is independent of the others. This is not true at high concentrations and $f_i < 1$. For very diluted concentrations, $f_i \approx 1$.

This measurement principle is applied by using a two electrode arrangement (Figure 6.26). One electrode includes the membrane that is selective to the ion of interest, and it contains a solution having a known concentration for ion species i . The other electrode is a reference, and all ions present in the sample to be measured can freely diffuse through its membrane. This arrangement involves several interfaces, but only one of them generates a variable potential: the one across the ion-selective membrane. From (6.46) we obtain

$$E = E_0 + \frac{RT}{zF} \ln a_i = E_0 + k \lg a_i \quad (6.50)$$

where a_i is now the activity for the ionic species of interest in the sample, and E_0 and k are constants. At 25°C , the sensitivity is 59.12 mV for each decade of variation in the change of activity for a monovalent cation, while at 100°C the sensitivity is 74.00 mV for each decade. It is therefore very important to know the cell temperature in order to correctly interpret the meaning of the measured potential difference. ISEs are bulky (100 mm to 150 mm in length and 10 mm in diameter), fragile, and require maintenance because the electrolyte is volatile.

When the quantity of interest is not the ionic activity but the concentration, from (6.49) and (6.50) we have

$$E = E_0 + k \lg f_i + k \lg C_i \quad (6.51)$$

If we assume that the activity coefficient is constant, then

$$E = E'_0 + k \lg f_i \quad (6.52)$$

Depending on the material for the membrane, there are different kinds of selective electrodes. Primary electrodes have a single membrane, which may be crystalline. When it is crystalline, it can be homogeneous or heterogeneous. In heterogeneous electrodes the crystalline material is mixed with a matrix of inert material. Crystalline membrane electrodes are applied to concentration measurement for F^- , Cl^- , Br^- , I^- , Cu^{2+} , Pb^{2+} , and Cd^{2+} , among others. The most common electrodes with a noncrystalline membrane are glass electrodes, like those used for pH and Na^+ measurement. Glass composition is chosen depending on the ion to be analyzed. Some metal salts have high electric conductivity and can be deposited on a metal electrode to act as electrolyte. These are termed *solid-state electrodes*. Other electrodes use a membrane (such as PVC or polyethylene) that includes an ion exchanger or a neutral material that transports the ion. K^+ , for example, is measured by valinomycin in a PVC membrane.

The most common double-membrane electrodes are gas electrodes. They include a porous membrane through which the gas to be analyzed diffuses and enters into a solution where the presence of the gas produces a change (e.g., in pH), which is the measured variable. This method is applied, for example, to concentration measurement for CO_2 , SO_2 , and NO_2 .

Output impedance for ISEs is very high, normally from $20\ M\Omega$ to $1\ G\Omega$, thus requiring electrometer amplifiers with very high input impedance (Section 7.2). Otherwise, current through the cell would imbalance the chemical reaction, leading to variation in its electric potential.

ISEs are used for concentration measurement in multiple applications where they have often replaced flame photometers. They are used, for example, in agriculture to analyze soils and fertilizers, in biomedical sciences and clinical laboratories for blood and urine analysis, in chemical and food industries, and in environmental monitoring to measure ambient pollution.

Solid electrolyte oxygen sensors rely on the influence that oxygen ions adsorbed by a metal oxide have on the concentration of charge carriers and, hence, on conductivity of the oxide—based on ions, hence it is an electrolyte. Oxygen molecules entering interstices in the oxide take two negative charges, so that two “holes” are created in order to keep the charge balance at zero. Oxygen molecules leaving interstices set two electrons free and create a vacancy for another oxygen molecule.

A common solid electrolyte for O_2 detection is yttrium-doped zirconia ($ZrO_2-Y_2O_3$) placed between two porous thick-film platinum electrodes, inside a temperature-controlled chamber at $600^\circ C$ to $850^\circ C$. The open-circuit output voltage is [17]

$$E = E_0 + \frac{RT}{4F} \ln \frac{(p_{O_2})_1}{(p_{O_2})_2} \quad (6.53)$$

$(p_{O_2})_1$ and $(p_{O_2})_2$ are the oxygen partial pressures inside and outside the

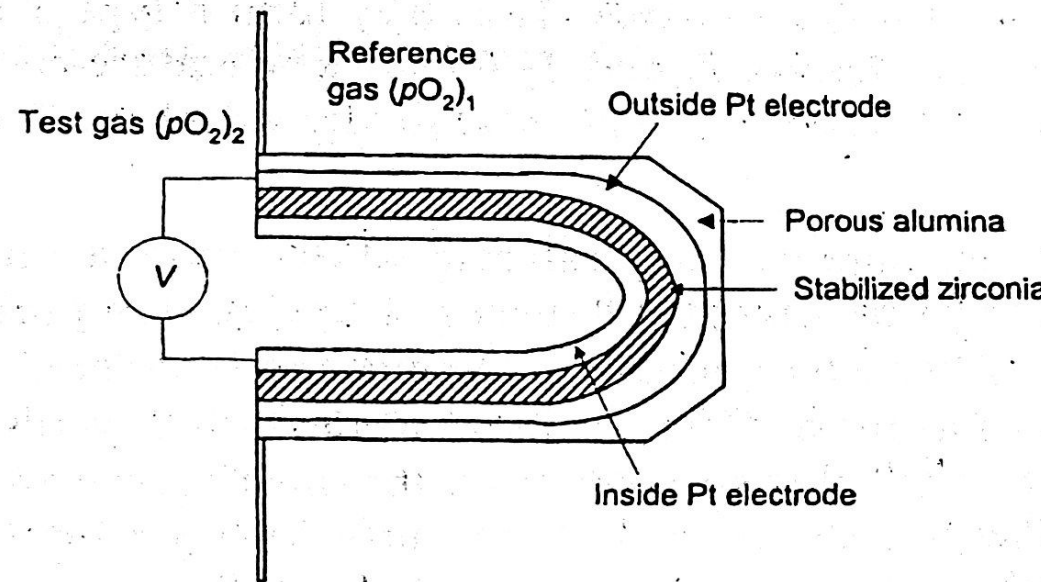


Figure 6.27 A potentiometric oxygen sensor generates a potential difference between electrodes on opposite sides of a stabilized zirconia membrane at high temperature.

example, air ($(p_{O_2})_2 = 21 \text{ kPa}$) (Figure 6.27)—from E we can determine $(p_{O_2})_1$ at a given temperature.

These sensors are fast and withstand temperatures from 600°C to 1200°C , but according to (6.53) they drift with temperature. They can be as small as 1 cm (length) by 2 mm (diameter). Because they consist of solid elements, their sensitivity to acceleration and vibration is minimal. Their main shortcomings are that they need a high temperature to work and that they have a low sensitivity to pressure changes: The voltage in (6.53) is proportional to the logarithm of the ratio between pressures, not to the pressure ratio. For this same reason, however, they can operate over a wide range of oxygen concentration. They are extensively used to determine the air-to-fuel ratio in internal combustion engines—for example, in automobiles, boilers, and furnaces.